



HHS Public Access

Author manuscript

Chemphyschem. Author manuscript; available in PMC 2018 March 01.

Published in final edited form as:

Chemphyschem. 2016 October 05; 17(19): 2962–2966. doi:10.1002/cphc.201600637.

Enhancing NMR Sensitivity of Natural-Abundance Low- γ Nuclei by Ultrafast Magic-Angle-Spinning Solid-State NMR Spectroscopy

Dr. Rongchun Zhang^a, Yitian Chen^b, Prof. Dr. Nair Rodriguez-Hornedo^b, and Prof. Dr. Ayyalusamy Ramamoorthy^a

^aBiophysics and Department of Chemistry, The University of Michigan, Ann Arbor, Michigan, 48109-1055 (USA)

^bDepartment of Pharmaceutical Science, The University of Michigan, Ann Arbor, Michigan, 48109-1055 (USA)

Abstract

Although magic-angle-spinning (MAS) solid-state NMR spectroscopy has been able to provide piercing atomic-level insights into the structure and dynamics of various solids, the poor sensitivity has limited its widespread application, especially when the sample amount is limited. Herein, we demonstrate the feasibility of acquiring high S/N ratio natural-abundance ^{13}C NMR spectrum of a small amount of sample (≈ 2.0 mg) by using multiple-contact cross polarization (MCP) under ultrafast MAS. As shown by our data from pharmaceutical compounds, the signal enhancement achieved depends on the number of CP contacts employed within a single scan, which depends on the $T_{1\rho}$ of protons. The use of MCP for fast 2D $^1\text{H}/^{13}\text{C}$ heteronuclear correlation experiments is also demonstrated. The significant signal enhancement can be greatly beneficial for the atomic-resolution characterization of many types of crystalline solids including polymorphic drugs and nanomaterials.

Keywords

cross-polarization; NMR spectroscopy; signal enhancement; structure elucidation; ultrafast MAS

Solid-state NMR spectroscopy has been playing very important roles by rendering substantial insights into the atomic-resolution molecular structures and dynamics of various types of solids including polymers,^[1,2] protein assemblies,^[3–8] bone,^[9–11] amyloid aggregates,^[12–15] and pharmaceutical compounds,^[16,17] However, its poor sensitivity has severely limited the application of this mighty technique. In fact, many exciting applications cannot utilize the benefits of sophisticated multidimensional solid-state NMR techniques. Use of a large sample quantity, longer data collection, modification of the sample to include specific isotopes or dopants, and/or data collection at cryogenic temperatures is mandatory for most solid-state NMR studies. Although a low temperature dynamic nuclear polarization

Correspondence to: Ayyalusamy Ramamoorthy.

Supporting Information for this article can be found under: <http://dx.doi.org/10.1002/cphc.201600637>.

(DNP) experiment^[18–21] can be used to enhance the sensitivity, there are issues with low spectral resolution, structural perturbation due to the inclusion of a polarizing agent, denaturing the sample due to freezing, and expense in carrying out the experiments. There is also considerable interest in developing proton-detection based techniques that can fully utilize the high gyromagnetic ratio and abundance of protons.^[22–30] However, in addition to the need for an additional frequency dimension, the resolution of low- γ nuclei spectrum obtained by proton detection can be compromised due to insufficient chemical shift evolution time in the indirect dimension. Therefore, there is still a need for methods to enhance the sensitivity of NMR experiments that utilize natural-abundance low- γ nuclei.

Heteronuclear cross-polarization (CP)^[31,32] has been widely employed in solid-state NMR experiments. Even though CP enhances the signal intensity of low- γ nuclei by a factor of γ_H/γ_X , the acquisition of natural-abundance ^{13}C signal is still a challenge when the sample quantity is limited. In the pioneering work by Pines et al.,^[31] multiple-contact CP (MCP) along with multiple acquisition was suggested to fully utilize the proton magnetization. However, to the best of our knowledge, such a pulse sequence has not been demonstrated to its full potential and is not practical under slow or moderate spinning speeds. On one hand, under moderate spinning speeds, high radio-frequency (RF) power continuous-wave (CW) irradiation has to be applied in order to spin-lock the proton magnetization as well as to achieve proton decoupling. On the other hand, the use of high-power CW will unavoidably reduce the number of CP contacts and signal acquisitions due to the probe duty cycle and potential sample heating. These problems could be well overcome by using low-power CW decoupling of protons under ultrafast MAS. In this study, we experimentally demonstrate the feasibility of using MCP to significantly enhance the signal intensity of natural-abundance ^{13}C nuclei under very fast MAS conditions. In addition to comparing the efficiencies of 1D MCP and the well-established ramp-CP^[33] experiments, we also demonstrate the use of MCP in 2D ^1H - ^{13}C heteronuclear correlation (HETCOR) experiments on small amounts (≈ 2.0 mg) of pharmaceutical compounds.

The 1D and 2D RF pulse sequences used in this study are shown in Figure 1. For experiments using MCP, as shown in Figure 1a, a double spin-lock with a ramp on the ^{13}C spin-lock followed by a CW proton decoupling during ^{13}C signal acquisition is repeated N times. At the end of final ^{13}C signal acquisition, a ^1H 90° pulse is applied to flip the remaining proton transverse magnetization to the $+z$ axis to accelerate the proton spin-lattice relaxation (T_1) process.^[34–36] Significant signal enhancement obtained using MCP at 60 kHz MAS is well demonstrated on a danazol/vanillin cocrystalline sample as shown in Figure 2. The effect of the last flip-back 90° pulse on the ^1H RF channel is demonstrated in Figure S1, where an additional $\approx 22\%$ signal enhancement is achieved. It should be noted that if the ^1H magnetization is decayed to zero after multiple CP contacts, then the final flip-back 90° pulse will have negligible effect on accelerating the T_1 relaxation of protons, as there is no residual transverse magnetization to flip back to the $+z$ axis. Details on the sample preparation, NMR experiments, theoretical explanation, and additional 2D $^1\text{H}/^{13}\text{C}$ HETCOR spectra are given in the Supporting Information.

Significant suppression of ^1H - ^1H dipolar couplings under 60 kHz MAS enhanced the efficiency of RF spin-locks of protons during MCP and resulted in a slow ^1H $T_{1\rho}$ relaxation

rate even when a weak RF field strength of ≈ 14 kHz was used for spin-locking protons. Because of the ability to retain proton transverse magnetization for a very long time, it is possible to utilize many CP contact blocks in the MCP experiment to acquire ^{13}C spectra with better sensitivity. As shown in Figure 2a, increasing the number of CP contacts (N) within each experimental scan, remarkably increased the ^{13}C signal-to-noise (S/N) ratio, needless to mention that the signal enhancement rendered by MCP is dramatic when compared to that obtained via the conventional ramp-CP as shown in Figure 2b. Indeed, only the aliphatic signals in the 10–60 ppm region could be observed in the conventional ramp-CP spectrum, and they are all very weak in intensity (Figure 2a). On the contrary, all the ^{13}C signals, including that of the quaternary carbons resonating in the 150–200 ppm region, could be clearly observed in the $\text{MCP}_{N=16}$ spectrum (Figure 2b). Due to the extremely long ^1H $T_{1\rho}$, the 16 FIDs obtained in the single scan have very similar intensity, as shown in Figure S2, which should result in an overall theoretical S/N ratio enhancement of 4.0 (Equation S7). A theoretical analysis of the S/N ratio enhancement is included in the Supporting Information. However, it is remarkable that the overall S/N ratio enhancement achieved by $\text{MCP}_{N=16}$ is ≈ 4.6 times as that obtained using ramp-CP, higher than the theoretical value of 4.0. This is because of the use of a ^1H flip-back 90° pulse after the final ^{13}C signal acquisition to accelerate ^1H T_1 relaxation. The efficiency of MCP is also further demonstrated on a different polymorphic compound, ibuprofen (Figure 3a,b), where all ^{13}C peak intensities are dramatically enhanced by MCP. In particular, as compared to conventional ramp-CP, the S/N ratio enhancement rendered by MCP for the peaks associated with quaternary carbons (C1, C4, and C7) are remarkably high. It is worth noting that the noise observed in the MCP spectrum is stronger than that of the conventional ramp-CP spectrum. Although we employed five CP contacts in the 1D MCP experiment, the signal decreased very fast due to ^1H $T_{1\rho}$ relaxation, and there was not much signal observed in the fourth and fifth FIDs (as shown in Figure S3). As a result, the S/N ratio is compromised by the superposition of fourth and fifth FIDs.

To further realize the advantage of MCP, it was incorporated into 2D ^{13}C - and ^1H -detected $^1\text{H}/^{13}\text{C}$ HETCOR experiments for sensitivity enhancement as shown in the RF pulse sequences given in Figure 1b and 1c. In the case of the ^{13}C -detected HETCOR experiment, ^1H chemical shifts are expressed during the incrementable t_1 period before repeating the CP- ^{13}C -acquisition block N times (Figure 1b). On the other hand, in the ^1H -detected HETCOR experiment, ^{13}C chemical shift is expressed during t_1 after the first CP and then following the z -filter the CP- ^1H -acquisition block is repeated N times as shown in Figure 1c. Therefore, these two types of HETCOR pulse sequences differ in the use of MCP: ^1H to ^{13}C CP (Figure 1b) versus ^{13}C to ^1H CP (Figure 1c).

The 2D ^{13}C -detected $^1\text{H}/^{13}\text{C}$ HETCOR spectra of danazol/vanillin co-crystals and ibuprofen are shown in Figures S4 and S5, respectively. Although significant signal enhancement could be achieved compared to the regular ^{13}C -detected HETCOR experiment, the proton spin diffusion during multiple CW decoupling periods may extend ^{13}C - ^1H correlations; an example is the case of danazol/vanillin co-crystals as shown in Figure S4b. The use of $N=20$ in the ^{13}C -detected HETCOR experiment resulted in a total CW decoupling duration of ≈ 120 ms. Though ^1H - ^1H dipolar couplings were largely suppressed by the ultrafast MAS as well as the spin-locking (reduces by half),^[1] the use of a very long total CW decoupling

duration can still allow the exchange of ^1H proton magnetization either through direct un-averaged ^1H - ^1H dipolar couplings (high-order homonuclear dipolar coupling terms) or via relayed polarization transfer. Then, the “exchanged” proton magnetization can further be transferred to nearby carbons in the successive CP periods. Because of this effect, most of the carbon resonances are correlated with proton resonances in the resultant 2D ^{13}C -detected MCP HETCOR spectra (Figure S4b). In contrast, when a small N value was used, such as the ^{13}C -detected MCP HETCOR spectrum of ibuprofen shown in Figure S5b, the total CW decoupling time was reduced to ≈ 28 ms and therefore the effect of spin diffusion was much reduced. As a result, only the non-bonded ^{13}C - ^1H correlations between aromatic carbon and aliphatic protons were observed in Figure S5b, while the ^{13}C - ^1H correlation between aromatic proton and aliphatic carbon is absent, which is due to the larger number of aliphatic protons than that of aromatic protons. Although proton spin diffusion is a major limitation for the ^{13}C -detected MCP HETCOR experiment, it might not be a problem for heavily deuterated samples, where the proton dipolar couplings can be completely averaged out by the ultrafast MAS. In such samples, the ^{13}C -detected MCP HETCOR spectrum can directly provide heteronuclear proximity information.

As mentioned above, the effect of proton spin diffusion in the ^{13}C -detected HETCOR experiment should be taken into account when employing a large number of CP-acquisition blocks. On the other hand, in the ^1H -detected MCP HETCOR experiment (Figure 1c), the ^{13}C spin diffusion can be safely ignored due to the very low natural-abundance of ^{13}C ($\approx 1\%$) as well as weak ^{13}C - ^{13}C couplings; and there is no role for \approx proton spin diffusion. As a result, the ^1H -detected MCP HETCOR experiment can greatly enhance the S/N ratio and also render the same information as that of a regular ^1H -detected HETCOR experiment but with enhanced sensitivity as demonstrated on ibuprofen (Figure 3) and danazol/vanillin cocrystal (Figure 4) samples.

As shown in Figures 3 and 4, the use of MCP significantly increases the S/N ratio of ^1H -detected HETCOR spectra. For ibuprofen sample, all the correlation signals are dramatically enhanced. However, due to the limited amount of ^{13}C magnetization from the initial single CP for the t_1 evolution (Figure 1c), the signals observed in the second and third FIDs were weaker than that observed in the first FID in the ^1H -detected MCP HETCOR experiment with $N=3$, because most of the ^{13}C magnetization has been transfer to ^1H in the first CP contact. However, the noise is constant in all the three FIDs. Therefore, the noise is a little high in the ^1H -detected MCP HETCOR spectrum in comparison to the regular HETCOR spectrum. However, for the ^1H -detected MCP HETCOR spectrum, an overall S/N ratio enhancement of $\approx 30\%$ is still achieved.

Similarly, signal enhancement was also achieved on the danazol/vanillin co-crystal sample (Figure 4). It is worth noting that resonances of most of the quaternary carbons (except C17 and C13) are absent in the regular HETCOR spectrum, because a contact time of 0.4 ms is too short to enable significant remote $^1\text{H} \rightarrow ^{13}\text{C}$ polarization transfer directly through the weak non bonded ^{13}C - ^1H dipolar couplings. However, in the ^1H -detected MCP HETCOR experiment, the ^{13}C magnetization remaining after the first ^{13}C to ^1H CP is transferred to proton in the subsequent CP contacts, and thus enhancing remote ^{13}C - ^1H correlations in the resultant 2D spectrum.

The experimental results presented above clearly demonstrate the significant signal enhancement by MCP that has considerable advantages for ^{13}C and other low- γ nuclei based solid-state NMR experiments under ultrafast MAS conditions. As shown by the experimental and theoretical (see the Supporting Information) analyses, the sensitivity enhancement rendered by MCP directly relies on the number of CP contacts (i.e. N) used in the experiment. As long as there is ^1H or ^{13}C magnetization remaining after the CW decoupling period, CP could further be applied for $^1\text{H} \rightarrow ^{13}\text{C}$ or $^{13}\text{C} \rightarrow ^1\text{H}$ polarization transfer, respectively. For natural-abundance samples, N is mainly determined by the proton relaxation time during the CP spin-lock and CW decoupling periods. Therefore, a system with a long ^1H $T_{1\rho}$ would allow the use of a very large number of CP contacts in the MCP experiment within the capability of the probe, and hence the feasibility of a dramatic enhancement of sensitivity; this is the case under ultrafast MAS as discussed below. It should also be mentioned that to avoid the loss of proton magnetization during decoupling periods, only CW decoupling can be used. The use of other decoupling schemes, such as the efficient composite-pulse based sequences, would destroy the ^1H magnetization. As a result, the CW decoupling power required to obtain high spectral resolution, which depends on the spinning speed of the sample, should be carefully optimized. Fortunately, ultrafast spinning speed does not require a high RF power for efficient decoupling^[38,39] and thus avoids potential sample heating. Indeed, MCP would be less rewarding under slow or moderate spinning speeds mainly because of the inefficiency of CW decoupling. These factors suggest that there are unique advantages of performing MCP based experiments under ultrafast spinning speeds (>100 kHz) in addition to the higher spectral resolution. For example, efficient suppression of dipolar couplings among protons by ultrafast MAS would: a) increase the $T_{1\rho}$ of protons and therefore enable the use of more CP-acquisition blocks in the pulse sequence to render higher sensitivity enhancement; b) enhance the CW decoupling efficiency and/or reduce the RF power required for decoupling.

We also note that there is another way to implement multiple-contact CP as used in the literature.^[40–43] In these published approaches, instead of signal acquisition immediately following the CP, the rare spin magnetization is generally stored along the $+z$ -axis for a delay of $\approx T_{1\text{H}}$ to enable the recovery of ^1H magnetization which then allows for the subsequent cross polarization from protons to rare nuclei. Although this approach enhances the signal intensity, the experimental time for each scan is longer than the MCP-based method presented in this study. In particular, for a heterogeneous sample with a broad range of ^{13}C T_1 values, a short T_{1z} filter delay between two neighboring CP periods will not be able to recover the lost ^1H magnetization during the previous CP, while a long T_{1z} filter delay will result in a significant signal loss (due to ^{13}C T_1 relaxation). Though other recent approaches that employed multiple acquisitions to utilize the residual magnetization of low- γ nuclei are valuable to obtain multiple 2D spectra of labeled biological solids, the number of acquisitions is quite limited by the initial signal-contact proton-enhanced CP.^[44,45] On the other hand, using the MCP approach proposed in this study could significantly broaden the benefits of such approaches under ultrafast MAS.

In conclusion, the dramatic enhancement of S/N ratio obtained in 1D ^{13}C CPMAS and ^1H or ^{13}C -detected 2D $^1\text{H}/^{13}\text{C}$ HETCOR experiments clearly demonstrated the feasibility of high-resolution natural-abundance ^{13}C based ultrafast MAS experiments on a small amount of

sample (≈ 2.0 mg). We foresee that the reported MCP approach will be valuable for a broad range of applications and the development of new techniques under ultrafast spinning speeds (>100 kHz). High-throughput characterization of pharmaceutical compounds by solid-state NMR and NMR crystallography studies would also be possible with the use of MCP under ultrafast MAS.

Supplementary Material

Refer to Web version on PubMed Central for supplementary material.

Acknowledgments

This work was supported by the funds from National Institutes of Health (GM084018 and GM095640 to A. R.).

References

1. Schmidt-Rohr, K., Spiess, HW. *Multidimensional Solid-State NMR and Polymers*. Academic Press; San Diego: 1994.
2. Hansen MR, Graf R, Spiess HW. *Chem Rev*. 2016; 116:1272–1308. [PubMed: 26312964]
3. Lu M, Hou G, Zhang H, Suiter CL, Ahn J, Byeon IJL, Perilla JR, Langmead CJ, Hung I, Gor'kov PL, et al. *Proc Natl Acad Sci USA*. 2015; 112:14617–14622. [PubMed: 26553990]
4. Carlon A, Ravera E, Hennig J, Parigi G, Sattler M, Luchinat C. *J Am Chem Soc*. 2016; 138:1601–1610. [PubMed: 26761154]
5. Can TV, Sharma M, Hung I, Gor'kov PL, Brey WW, Cross TA. *J Am Chem Soc*. 2012; 134:9022–9025. [PubMed: 22616841]
6. Park SH, Das BB, Casagrande F, Tian Y, Nothnagel HJ, Chu M, Kiefer H, Maier K, De Angelis AA, Marassi FM, Opella SJ. *Nature*. 2012; 491:779–783. [PubMed: 23086146]
7. Weingarth M, Baldus M. *Acc Chem Res*. 2013; 46:2037–2046. [PubMed: 23586937]
8. Wang S, Munro RA, Shi L, Kawamura I, Okitsu T, Wada A, Kim SY, Jung KH, Brown LS, Ladizhansky V. *Nat Methods*. 2013; 10:1007–1012. [PubMed: 24013819]
9. Hu YY, Rawal A, Schmidt-Rohr K. *Proc Natl Acad Sci USA*. 2010; 107:22425–22429. [PubMed: 21127269]
10. Duer MJ. *J Magn Reson*. 2015; 253:98–110. [PubMed: 25797009]
11. Xu J, Zhu P, Gan Z, Sahar N, Tecklenburg M, Morris MD, Kohn DH, Ramamoorthy A. *J Am Chem Soc*. 2010; 132:11504–11509. [PubMed: 20681578]
12. Petkova AT, Ishii Y, Balbach JJ, Antzutkin ON, Leapman RD, Delaglio F, Tycko R. *Proc Natl Acad Sci USA*. 2002; 99:16742–16747. [PubMed: 12481027]
13. Linser R, Sarkar R, Krushelnitzky A, Mainz A, Reif B. *J Biomol NMR*. 2014; 59:1–14. [PubMed: 24595988]
14. Patel HR, Pithadia AS, Brender JR, Fierke CA, Ramamoorthy A. *J Phys Chem Lett*. 2014; 5:1864–1870. [PubMed: 26273866]
15. Prade E, Bittner HJ, Sarkar R, Lopez del Amo JM, Althoff-Ospelt G, Multhaup G, Hildebrand PW, Reif B. *J Biol Chem*. 2015; 290:28737–28745. [PubMed: 26416887]
16. Harris RK. *J Pharm Pharmacol*. 2007; 59:225–239. [PubMed: 17270076]
17. Chattah AK, Zhang R, Mroue KH, Pfund LY, Longhi MR, Ramamoorthy A, Garner C. *Mol Pharm*. 2015; 12:731–741. [PubMed: 25584993]
18. Tycko R. *Acc Chem Res*. 2013; 46:1923–1932. [PubMed: 23470028]
19. Maly T, Debelouchina GT, Bajaj VS, Hu KN, Joo CG, Mak-Jurkauskas ML, Sirigiri JR, van der Wel PCA, Herzfeld J, Temkin RJ, et al. *J Chem Phys*. 2008; 128:052211. [PubMed: 18266416]
20. Rossini AJ, Zagdoun A, Lelli M, Lesage A, CopØret C, Emsley L. *Acc Chem Res*. 2013; 46:1942–1951. [PubMed: 23517009]

21. Akbey, Ü., Franks, WT., Linden, A., Orwick-Rydmark, M., Lange, S., Oschkinat, H. *Hyperpolarization Methods NMR Spectrosc.* Springer; Berlin: 2013. p. 181-228.
22. Ishii Y, Yesinowski JP, Tycko R. *J Am Chem Soc.* 2001; 123:2921–2922. [PubMed: 11456995]
23. Asami S, Rakwalska-Bange M, Carlomagno T, Reif B. *Angew Chem Int Ed.* 2013; 52:2345–2349. *Angew Chem.* 2013; 125:2401–2405.
24. Zhang R, Ramamoorthy A. *J Chem Phys.* 2016; 144:034202. [PubMed: 26801026]
25. Barbet-Massin E, Pell AJ, Retel J, Andreas LB, Jaudzems K, Franks WT, Nieuwkoop AJ, Hiller M, Higman VA, Guerry P, et al. *J Am Chem Soc.* 2014; 136:12489–12497. [PubMed: 25102442]
26. Kobayashi T, Mao K, Paluch P, Nowak-Król A, Sniechowska J, Nishiyama Y, Gryko DT, Potrzebowski MJ, Pruski M. *Angew Chem Int Ed.* 2013; 52:14108–14111. *Angew Chem.* 2013; 125:14358–14361.
27. Zhang R, Pandey MK, Nishiyama Y, Ramamoorthy A. *Sci Rep.* 2015; 5:11810. [PubMed: 26138791]
28. Wang S, Parthasarathy S, Xiao Y, Nishiyama Y, Long F, Matsuda I, Endo Y, Nemoto T, Yamauchi K, Asakura T, Takeda M, Terauchi T, Kainosho M, Ishii Y. *Chem Commun.* 2015; 51:15055–15058.
29. Nishiyama Y, Malon M, Ishii Y, Ramamoorthy A. *J Magn Reson.* 2014; 244:1–5. [PubMed: 24801998]
30. Kulminkaya N, Vasa SK, Giller K, Becker S, Kwan A, Sunde M, Linser R. *Chem Commun.* 2016; 52:268–271.
31. Pines A, Gibby MG, Waugh JS. *J Chem Phys.* 1973; 59:569.
32. Schaefer J, Stejskal EO. *J Am Chem Soc.* 1976; 98:1031–1032.
33. Metz G, Wu X, Smith SO. *J Magn Reson Ser A.* 1994; 110:219–227.
34. Tegenfeldt J, Haeberlen U. *J Magn Reson.* 1979; 36:453–457.
35. a) Saito K, Martineau C, Fink G, Taulelle F. *Solid State Nucl Magn Reson.* 2011; 40:66–71. [PubMed: 21641189] b) Lopez JJ, Kaiser C, Asami S, Glaubitz C. *J Am Chem Soc.* 2009; 131:15970–15971. [PubMed: 19886687]
36. Demers JP, Vijayan V, Lange A. *J Phys Chem B.* 2015; 119:2908–2920. [PubMed: 25588120]
37. Choudhary MI, Atta-Ur-Rahman Azizuddin. *Nat Prod Lett.* 2002; 16:101–106. [PubMed: 11990425]
38. Kotecha M, Wickramasinghe NP, Ishii Y. *Magn Reson Chem.* 2007; 45:S221–S230. [PubMed: 18157841]
39. Madhu PK. *Isr J Chem.* 2014; 54:25–38.
40. Tang W, Nevzorov AA. *J Magn Reson.* 2011; 212:245–248. [PubMed: 21784682]
41. Nevzorov AA. *J Magn Reson.* 2011; 209:161–166. [PubMed: 21296016]
42. Johnson RL, Schmidt-Rohr K. *J Magn Reson.* 2014; 239:44–49. [PubMed: 24374751]
43. Gerstein, BC., Dybowski, CR. *Transient Techniques in NMR of Solids: an Introduction to Theory and Practice.* Academic Press; San Diego: 1985.
44. Gopinath T, Mote KR, Veglia G. *J Biomol NMR.* 2015; 62:53–61. [PubMed: 25749871]
45. Gopinath T, Veglia G. *Angew Chem Int Ed.* 2012; 51:2731–2735. *Angew Chem.* 2012; 124:2785–2789.

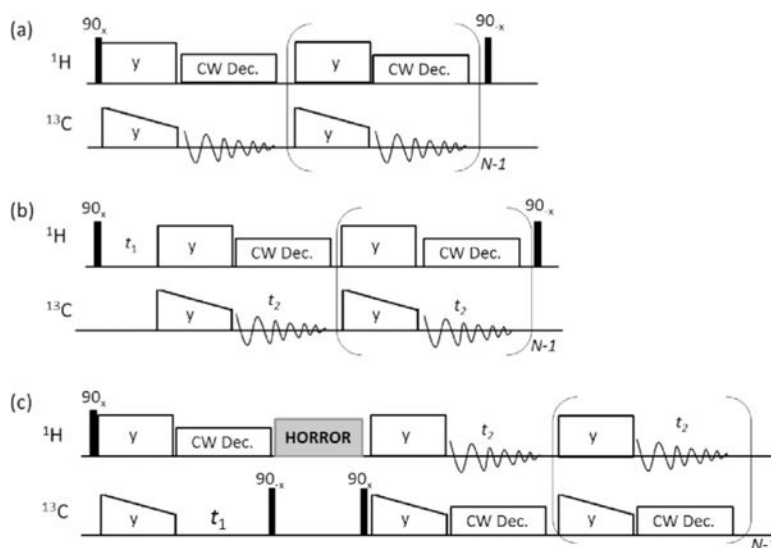


Figure 1. Multiple-contact CP (MCP) based NMR pulse sequences. a) 1D MCP experiment for recording natural-abundance 1D ^{13}C spectrum. b) ^{13}C -detected MCP 2D $^1\text{H}/^{13}\text{C}$ HETCOR experiment. c) ^1H -detected MCP 2D $^1\text{H}/^{13}\text{C}$ HETCOR experiment. The final 90° pulse (in a and b) was used to flip the remaining ^1H transverse magnetization back to the $+z$ axis to enhance the T_1 relaxation of protons.

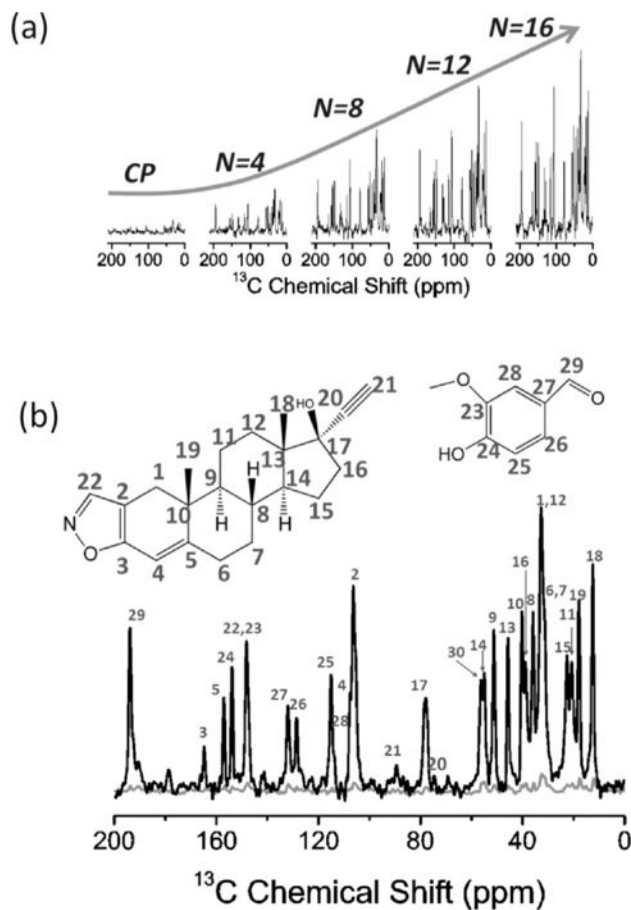


Figure 2.

Natural-abundance ^{13}C NMR spectra of danazol/vanillin co-crystalline sample. a) Comparison of spectra obtained by conventional ramp-CP and MCP with the indicated number (N) of CP contacts. b) Comparison of spectra obtained with conventional ramp-CP (grey) and MCP with $N=16$ (black). The molecular structure and resonance assignment are shown on top of the spectrum in (b) according to the work of Atta-Ur-Rahman et al.^[37] A linear ramp of 28% was applied on all the ^{13}C spin-lock RF pulses as shown in Figure 1. Other experimental parameters used to obtain the spectra are: 60 kHz MAS, CP contact time of 1 ms, 6 ms data acquisition time, 2100 scans, 14 kHz decoupling and 10 s recycle delay. The total experimental time was ≈ 5.9 hours for each spectrum. A 600 MHz Agilent solid-state NMR spectrometer and a 1.2 mm triple-resonance MAS probe were used. The ^1H and ^{13}C resonance frequencies were 599.8 and 150.8 MHz, respectively.

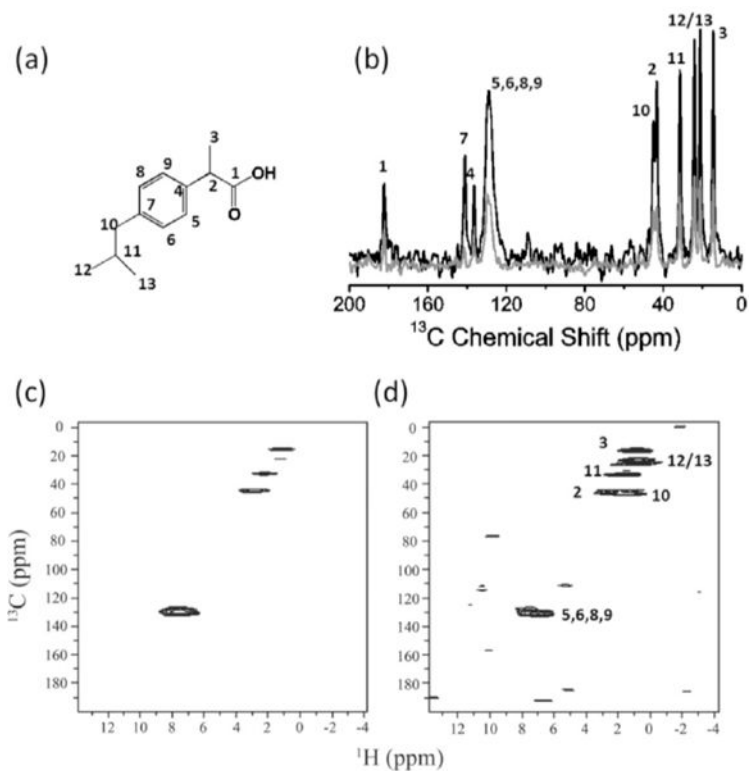


Figure 3. Natural-abundance 1D and 2D NMR spectra of ibuprofen powder. a) Chemical structure of ibuprofen. b) Comparison of spectra obtained using conventional ramp-CP (grey) and MCP with $N=5$ (black). Other experimental parameters used to obtain the spectra are: 60 kHz MAS, 1 ms CP contact time, 7 ms acquisition time, 1200 scans, 14 kHz proton decoupling and 4 s recycle delay. The total experimental time was ≈ 1.8 hours for each spectrum. c,d) ^1H -detected HETCOR spectra of ibuprofen obtained using the pulse sequence shown in Figure 1c with $N=1$ and $N=3$, respectively. The initial $^1\text{H} \rightarrow ^{13}\text{C}$ CP contact time was 2.0 ms, and each $^{13}\text{C} \rightarrow ^1\text{H}$ CP contact time was 0.4 ms. Other experimental parameters include 7 ms of each signal acquisition, 3 s recycle delay, and 20 scans for each t_1 increment.

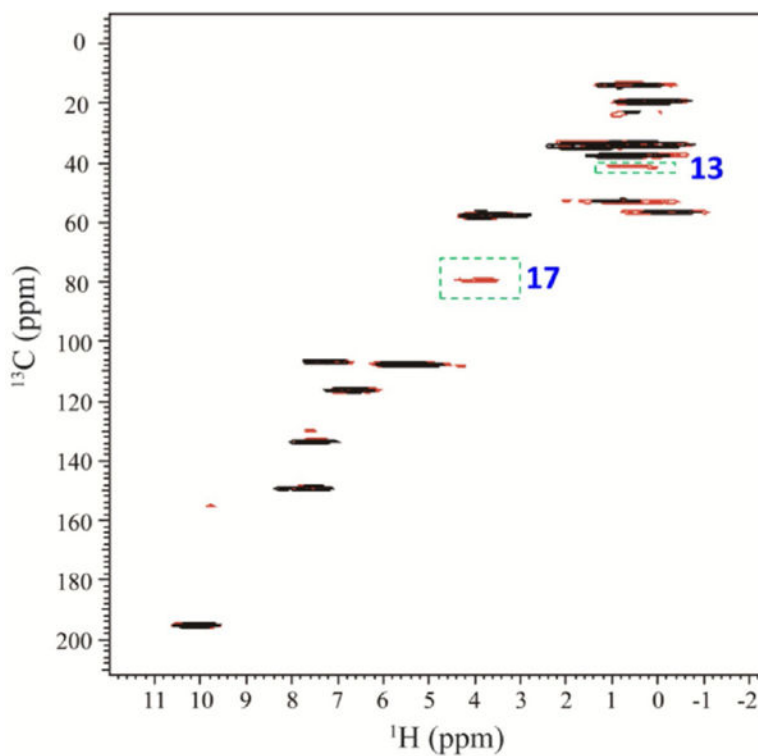


Figure 4.

^1H -detected 2D $^1\text{H}/^{13}\text{C}$ HETCOR spectrum of danazol/vanillin co-crystals obtained using the pulse sequence shown in Figure 1c with $N=1$ (black) and $N=3$ (red). The initial $^1\text{H} \rightarrow ^{13}\text{C}$ CP contact time was 2.0 ms, and each $^{13}\text{C} \rightarrow ^1\text{H}$ CP contact time was 0.4 ms. Other experimental parameters include 6 ms of each signal acquisition, 7 s recycle delay, and 36 scans for each t_1 increment.